A Tonoplast-Associated Calcium-Signaling Module Dampens ABA Signaling during Stomatal Movement[1]

Shi-Jian Song,[a] Qiang-Nan Feng,[a] Chun-Long Li,[b] En Li,[a] Qi Liu,[a] Hui Kang,[a] Wei Zhang,[b] Yan Zhang,[a] and Sha Li[a,2]

[a]State Key Laboratory of Crop Biology, College of Life Sciences, Shandong Agricultural University, Tai'an 271018, China

[b]The Key Laboratory of Plant Cell Engineering and Germplasm Innovation, Ministry of Education, School of Life Science, Shandong University, Jinan 250100, China

ORCID IDs: 0000-0002-6077-9138 (W.Z.); 0000-0002-3501-5857 (Y.Z.); 0000-0002-7197-0181 (S.L.)

Stomatal movement, critical for photobiosynthesis, respiration, and stress responses, is regulated by many factors, among which abscisic acid (ABA) is critical. Early events of ABA signaling involve Ca^{2+} influx and an increase of cytoplasmic calcium ($[Ca^{2+}]_{cyt}$). Positive regulators of this process have been extensively studied, whereas negative regulators are obscure. ABA-induced stomatal closure involves K^+ flux and vacuolar convolution. How these processes are connected with Ca^{2+} is not fully understood. We report that *pat10-1*, a null mutant of Arabidopsis (*Arabidopsis thaliana*) *PROTEIN S-ACYL TRANSFERASE10* (*PAT10*), is hypersensitive to ABA-induced stomatal closure and vacuolar convolution. A similar phenotype was observed in *cbl2;cbl3*, the double mutant of CBL2 and CBL3, whose tonoplast association depends on PAT10. Functional loss of the PAT10-CBL2/CBL3 system resulted in enhanced Ca^{2+} influx and $[Ca^{2+}]_{cyt}$ elevation. Promoting vacuolar K^+ accumulation by overexpressing *NHX2* suppressed ABA-hypersensitive stomatal closure and vacuolar convolution of the mutants, suggesting that PAT10-CBL2/CBL3 positively mediates vacuolar K^+ accumulation. We have identified CBL-interacting protein kinases (CIPKs) that mediate CBL2/CBL3 signaling during ABA-induced stomatal movement. Functional loss of the PAT10-CBL2/3-CIPK9/17 system in guard cells enhanced drought tolerance. We propose that the tonoplast CBL-CIPK complexes form a signaling module that negatively regulates ABA signaling during stomatal movement.

The stomatal pore is surrounded by two guard cells in the epidermis of plant leaves and plays crucial roles in maintaining a sustainable environment by mediating water use efficiency, photobiosynthesis, and responses to biotic and abiotic stresses of terrestrial plants (Hetherington, 2001; Hauser et al., 2011). Stomatal movement serves as an excellent system to study fundamental phenomena, such as cellular responses to environmental stimuli, ion homeostasis, and endomembrane dynamics (Hetherington, 2001; Kim et al., 2010; Kollist et al., 2014). Environmental cues, including light conditions, CO_2 concentration, humidity, and most importantly, the phytohormone abscisic acid (ABA), all affect stomatal movement (Hetherington, 2001; Kim et al., 2010; Hauser et al., 2011).

ABA promotes stomatal closure and inhibits light-induced stomatal opening (Hetherington, 2001; Kim et al., 2010; Finkelstein, 2013). One of the key events downstream of ABA in stomatal movement is Ca^{2+} influx from the plasma membrane (PM; Blatt, 2000; Pei et al., 2000; Himmelbach et al., 2003; Kim et al., 2010; Zhang et al., 2011). The elevation of Ca^{2+} in the cytoplasm ($[Ca^{2+}]_{cyt}$) initiates signaling through Ca^{2+} sensors, i.e. proteins with Ca^{2+}-binding domains, such as calcium dependent protein kinases, which positively regulate Ca^{2+}-mediated ABA signaling (Pei et al., 2000; Mori et al., 2006; Zhang et al., 2011; Ye et al., 2013; Brandt et al., 2015; Zou et al., 2015).

Stomatal movement accompanies dynamic vacuolar remodeling (Gao et al., 2005; Tanaka et al., 2007). By fluorescent labeling, pharmacological and genetic interference, and confocal imaging, it was shown that vacuolar fragmentation, or convolution, is a crucial event for stomatal closure (Gao et al., 2005; Tanaka et al., 2007; Bak et al., 2013; Andrés et al., 2014). Changes in vacuolar volume due to dynamic vacuolar remodeling result in alterations in guard cell turgor and are crucial for stomatal movement (Gao et al., 2005; Tanaka et al., 2007; Bak et al., 2013; Andrés et al., 2014). Turgor regulation requires K^+ fluxes at the PM and the tonoplast (Gobert et al., 2007; MacRobbie and Smyth, 2010; Bassil et al., 2011; Barragán et al., 2012;

[1]This research was supported by Natural Science Foundation of China (31471304 and 31625003 to Y.Z.), Shandong Provincial Natural Science Foundation (ZR2014CM027 to S.L.), and the Opening Scientific Program of the State Key Laboratory of Plant Physiology and Biochemistry, China Agricultural University (SKLPPBKF1804 to S.L.). Y.Z.'s laboratory is partially supported by the Tai-Shan Scholar Program, Shandong Provincial Government.

[2]Address correspondence to shali@sdau.edu.cn.

The author responsible for distribution of materials integral to the findings presented in this article in accordance with the policy described in the Instructions for Authors (www.plantphysiol.org) is: Sha Li (shali@sdau.edu.cn).

S.-J.S. performed most of the experiments and acquired and analyzed the data with the assistance of Q.-N.F.; C.-L.L. and W.Z. performed the whole-cell patch clamping and analyzed the data; E.L. performed the in vitro pull-down assay; S.L. conceived the project; S.L. and Y.Z. analyzed the data and wrote the article.

www.plantphysiol.org/cgi/doi/10.1104/pp.18.00377

Andrés et al., 2014). Transporters of K^+ have been identified, and their mutation often results in defective stomatal movement (Gobert et al., 2007; Barragán et al., 2012; Andrés et al., 2014).

Signaling pathways require negative feedback to avoid uncontrolled signal amplification. A major class of Ca^{2+} decoders, calcineurin B-like proteins (CBLs), interact with and activate CBL-interacting protein kinases (CIPKs) to relay Ca^{2+} signaling (Guo et al., 2001; Gong et al., 2004; Kolukisaoglu et al., 2004; Luan, 2009). CBL-CIPK complexes are associated with the PM or the tonoplast (Gong et al., 2004; Batistic et al., 2010; Tang et al., 2012, 2015; Liu et al., 2013). Several PM-associated CBLs and their interacting CIPKs were suggested to act as "brakes" in ABA signaling, as their mutation resulted in hypersensitivity to ABA during seed germination (Guo et al., 2002; Pandey et al., 2004, 2008; D'Angelo et al., 2006) and stomatal movement (Cheong et al., 2007). However, little is known about the role of CBL-CIPKs at the tonoplast, another important signaling platform, in ABA signaling.

We showed previously that the tonoplast association of Arabidopsis (Arabidopsis thaliana) CBL2 and CBL3 depends on the protein *S*-acyl transferase (PAT) activity of PAT10 (Zhou et al., 2013). Here, we demonstrate that loss of *PAT10* function results in ABA hypersensitivity during stomatal movement. ABA-induced Ca^{2+} influx and $[Ca^{2+}]_{cyt}$ elevation were both enhanced in *pat10-1*, a null mutant of *PAT10*. The double mutant of *CBL2* and *CBL3*, *cbl2;cbl3*, phenocopied *pat10-1* in ABA hypersensitive stomatal movement. Stomatal closure in *pat10-1* and *cbl2;cbl3* accompanied hypersensitive vacuolar convolution. We further show that enhancing vacuolar accumulation of K^+ by overexpressing the Na^+,K^+/H^+ antiporter NHX2 suppresses the hypersensitivity of the mutants to ABA, suggesting that PAT10-CBL2/CBL3 mediate K^+ homeostasis at the tonoplast. Furthermore, we identified two CIPKs that mediate CBL2/CBL3 signaling in guard cells. In addition, functional loss of the PAT10-CBL2/3-CIPK9/17 system in guard cells enhanced drought tolerance. Finally, we propose that the tonoplast CBL-CIPK complexes form a signaling module, negatively regulating ABA signaling during stomatal movement.

RESULTS

PAT10 Loss of Function Results in ABA-Hypersensitive Stomatal Movement

Previously, we demonstrated that the tonoplast association of CBL2 and CBL3 depends on PAT10 (Zhou et al., 2013; Zhang et al., 2015). *PAT10* showed strong expression in guard cells by promoter-reporter analysis (Zhou et al., 2013), as well as by a guard cell-specific transcriptomic study (Bates et al., 2012). We therefore hypothesized that PAT10 might play a role in stomatal movement. Indeed, the null mutant of *PAT10*, *pat10-1*, was hypersensitive to ABA-induced stomatal closure (Fig. 1, A and D) and ABA inhibition of light-induced stomatal opening (Fig. 1, B and E). By contrast, light-induced stomatal opening was not affected in *pat10-1* (Fig. 1, C and F). These results suggested that PAT10 plays a negative role in ABA signaling during stomatal movement.

To exclude the possibility that the expression of *PAT10* in cells other than guard cells affected stomatal movement, we generated *PAT10* gain-of-function and loss-of-function transgenic plants using Pro_{GC1}, a guard cell-specific promoter (Yang et al., 2008). More than 20 individual Pro_{GC1}:PAT10-RNAi and Pro_{GC1}:PAT10-mRFP lines were obtained and they showed consistent results. RNA interference (RNAi) of *PAT10* specifically in guard cells substantially reduced the expression of *PAT10g-GFP* (Supplemental Fig. S1), indicating the efficiency of the Pro_{GC1}:PAT10-RNAi construct. Confocal laser scanning microscopy of leaves from Pro_{GC1}:PAT10-mRFP transgenic plants confirmed exogenous expression of *PAT10* in guard cells (Supplemental Fig. S1). We found that the Pro_{GC1}:PAT10-RNAi transgenic plants were hypersensitive whereas the Pro_{GC1}:PAT10-mRFP transgenic plants were hyposensitive to ABA-induced stomatal closure (Supplemental Fig. S1). Down-regulating *PAT10* specifically in guard cells mimicked the ABA hypersensitive stomatal movement seen in *pat10-1*, while enhanced expression of *PAT10* in guard cells had the opposite effect (Supplemental Fig. S1). These results indicated that PAT10 functions in a cell-autonomous way to negatively mediate ABA signaling during stomatal movement.

The *cbl2;cbl3* Double Mutant Mimics *pat10-1* in ABA-Hypersensitive Stomatal Movement

Because PAT10 functions through substrate *S*-acylation (Zhou et al., 2013), we reasoned that the ABA hypersensitivity of *pat10-1* was due to failed *S*-acylation of its substrates. The *S*-acylation-dependent tonoplast localization of CBL2 and CBL3 relies on PAT10 (Zhou et al., 2013; Zhang et al., 2015) and the developmental defects of the *PAT10* loss-of-function mutant (Zhou et al., 2013) are similar to those of the *cbl2;cbl3* double mutant (Tang et al., 2012). We thus hypothesized that the ABA hypersensitive stomatal movement of *pat10-1* was due to functional defects of CBL2 and CBL3. Indeed, both *CBL2* and *CBL3* are expressed in guard cells based on promoter:GUS analyses (Tang et al., 2012; Liu et al., 2013) and guard cell-specific microarray analysis (Bates et al., 2012). To test this hypothesis, we analyzed stomatal movement of the *cbl2;cbl3* double mutant (Tang et al., 2012). Indeed, *cbl2;cbl3* was hypersensitive to ABA-induced stomatal closure (Fig. 2, A and D) and ABA inhibition of light-induced stomatal opening (Fig. 2, B and E), but not light-induced stomatal opening (Fig. 2, C and F). Mutations at either *CBL2* or *CBL3* did not affect stomatal movement significantly (Supplemental Fig. S2). The phenotypic resemblance of *pat10-1* and *cbl2;cbl3* is consistent with the observation that the tonoplast association of CBL2 was abolished in *pat10-1*

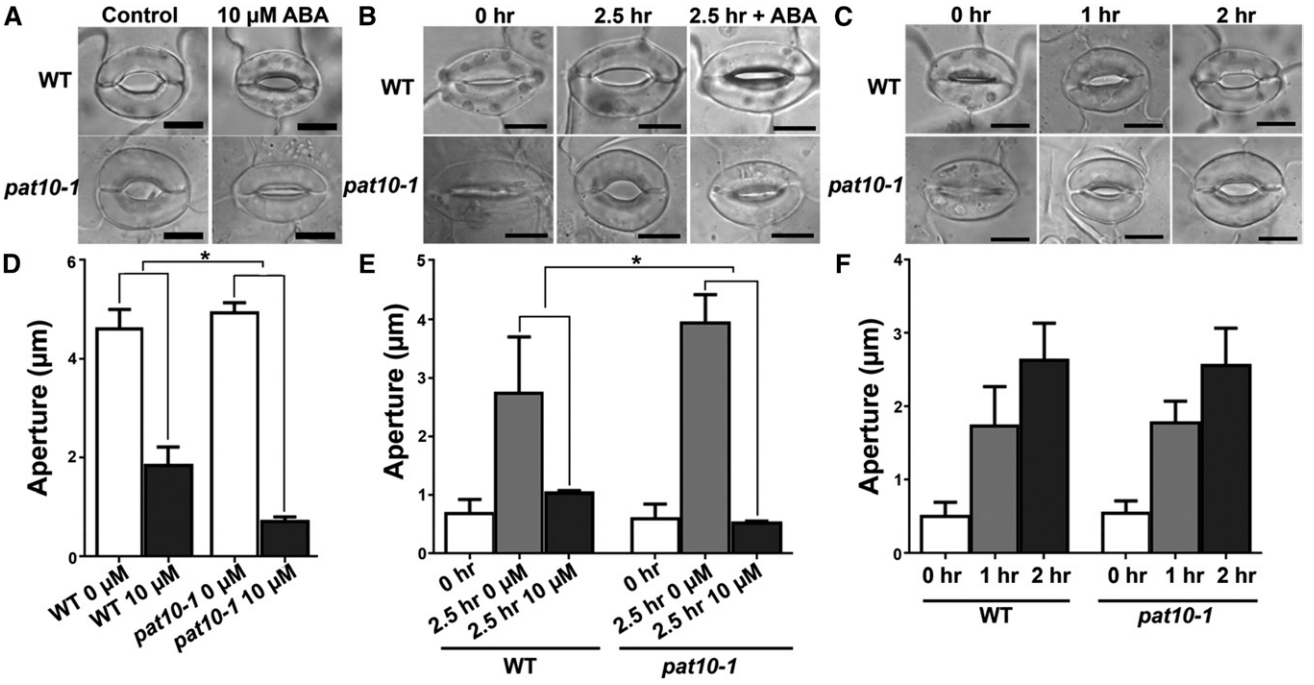

Figure 1. *PAT10* loss-of-function resulted in ABA hypersensitivity during stomatal movement. A to C, Representative wild type or *pat10-1* stomata for ABA-induced stomatal closure (A), for ABA inhibition of light-induced stomatal opening (B), or for light-induced stomatal opening (C). D, ABA-induced stomatal closure in the wild type and *pat10-1*. Rosette leaves with preopened stomata were treated with 0 or 10 μM ABA for 2 h before the apertures were measured. E, ABA inhibition of light-induced stomatal opening in the wild type and *pat10-1*. Rosette leaves with preclosed stomata (0 h) were illuminated for 2.5 h with (2.5 h 10 μM) or without 10 μM ABA (2.5 h 0 μM) before the apertures were measured. F, Light-induced stomatal opening in the wild type and *pat10-1*. Rosette leaves with preclosed stomata were illuminated for designated time points before the apertures were measured. Results in D to F are means ± SE (n = 3). Each experiment includes 30 stomata from three epidermal peels. Asterisks indicate significant difference (t test, $P < 0.05$). Bars = 10 μm for A to C.

guard cells (Supplemental Fig. S3). These results suggest that PAT10 mediates the tonoplast localization of CBL2 and CBL3 and that tonoplast-localized CBL2 and CBL3 are negative regulators of the ABA response during stomatal movement.

Functional Loss of *PAT10* or *CBL2* and *CBL3* Results in Hypersensitivity to ABA-Induced Ca^{2+} Influx

Ca^{2+} influx and $[Ca^{2+}]_{cyt}$ increase are among earliest events during ABA signaling, whereas CBL2 and CBL3 are able to decode Ca^{2+} signal. The hypersensitivity of *pat10-1* and *cbl2;cbl3* to ABA-induced stomatal closure suggested that they form a negative feedback loop on Ca^{2+}-mediated ABA signaling. Although ABA-induced Ca^{2+} influx initially comes from the PM, we reasoned that changes in tonoplast Ca^{2+} sensors would affect Ca^{2+} influx at the PM by perturbing Ca^{2+} homeostasis, as previously proposed (Batistic et al., 2010; Pittman, 2012).

To test our hypothesis, we examined ABA-induced Ca^{2+} influx in guard cells under the rationale that the impairment of a negative feedback loop would result in an enhanced Ca^{2+} influx. We performed patch-clamp analysis (Pei et al., 2000; Mori et al., 2006; Zhang et al., 2008, 2011) to determine Ca^{2+} currents at the PM. Both *pat10-1* and *cbl2;cbl3* were comparable to the wild type without ABA treatment; however, they were hypersensitive to ABA-induced Ca^{2+} influx (Fig. 3, A-D). To verify that Ca^{2+} influx upon ABA treatment was enhanced in *pat10-1* and *cbl2;cbl3*, we took a pharmacological approach by applying $LaCl_3$, a potent Ca^{2+} channel blocker. Simultaneous application of $LaCl_3$ and ABA suppressed the ABA hypersensitivity of *pat10-1* and *cbl2;cbl3* (Fig. 3E), suggesting that Ca^{2+} influx at the PM upon ABA treatment is enhanced in *pat10-1* and *cbl2;cbl3*.

To exclude the possibility that $LaCl_3$ treatment affected processes other than Ca^{2+} signaling and to provide evidence that elevated $[Ca^{2+}]_{cyt}$ contributed to ABA hypersensitive stomatal closure of *pat10-1* and *cbl2;cbl3*, we first introduced cytoplasmic aequorin (Mehlmer et al., 2012) into the mutants. Aequorin is a genetically encoded luminescent calcium indicator that emits light directly upon calcium binding (Mehlmer et al., 2012). Consistent with the ABA-hypersensitive stomatal closure (Figs. 1 and 2), *pat10-1* and *cbl2;cbl3* showed hypersensitivity to ABA-induced $[Ca^{2+}]_{cyt}$ elevation (Fig. 3F). Next, we applied EGTA, which chelates extracellular Ca^{2+} from the medium and thus compromises $[Ca^{2+}]_{cyt}$

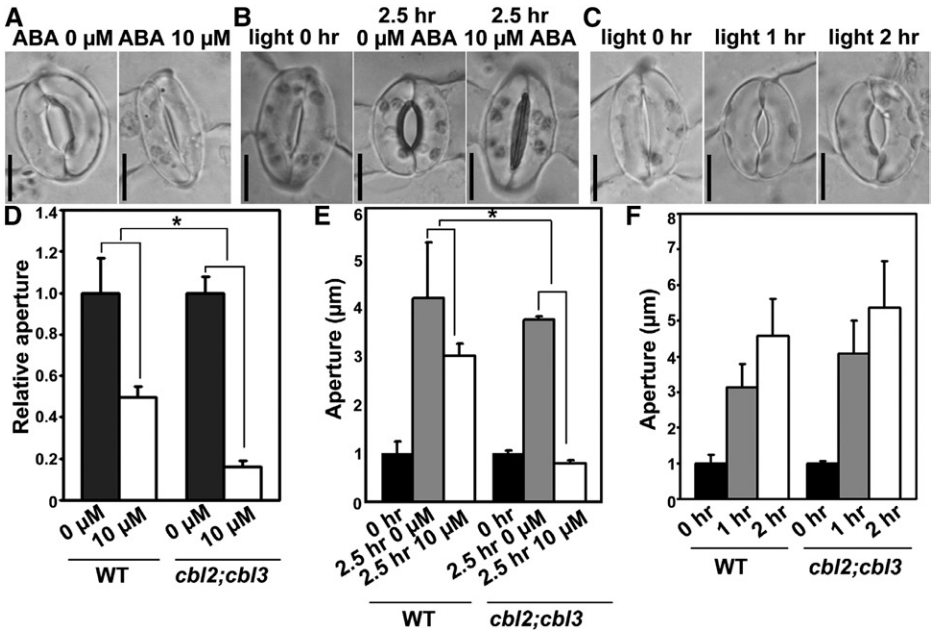

Figure 2. The *cbl2;cbl3* double mutant is hypersensitive to ABA during stomatal movement. A to C, Representative *cbl2;cbl3* stomata for ABA-induced stomatal closure (A), for ABA-inhibition of light-induced stomatal opening (B), or for light-induced stomatal opening (C). D, ABA-induced stomatal closure in the wild type and *cbl2;cbl3*. Rosette leaves with preopened stomata were treated with 0 or 10 μM ABA for 2 h before the apertures were measured. E, ABA inhibition of light-induced stomatal opening in the wild type and *cbl2;cbl3*. Rosette leaves with preclosed stomata (0 h) were illuminated for 2.5 h with (2.5 h/10 μM) or without 10 μM ABA (2.5 h/0 μM) before the apertures were measured. F, Light-induced stomatal opening in the wild type and *cbl2;cbl3*. Rosette leaves with preclosured stomata were illuminated for designated time points before the apertures were measured. Results in D to F are means ± SE ($n = 3$). Each experiment includes 30 stomata from three epidermal peels. Asterisks indicate significant difference (*t* test, $P < 0.05$). Bars = 10 μm for A to C.

signaling. Application of EGTA similarly suppressed the ABA hypersensitive stomatal closure of *pat10-1* and *cbl2;cbl3* (Supplemental Fig. S4). These results suggested that ABA induces enhanced Ca^{2+} influx in *pat10-1* and *cbl2;cbl3* and that elevated $[Ca^{2+}]_{cyt}$ contributed to the ABA hypersensitive stomatal closure of *pat10-1* and *cbl2;cbl3.* Because CBL2 and CBL3 are sensors of $[Ca^{2+}]_{cyt}$, it implies that PAT10-CBL2/CBL3 serves as a negative feedback loop to dampen Ca^{2+}-mediated ABA signaling during stomatal closure.

Mutations in *PAT10* and *CBL2*/*CBL3* Result in Hypersensitivity to ABA-Induced Vacuolar Convolution

Because stomatal movement is driven by vacuolar turgor (Gao et al., 2005; Tanaka et al., 2007; Bak et al., 2013; Andrés et al., 2014; Kollist et al., 2014) and PAT10-CBL2/CBL3 are associated with the tonoplast (Zhou et al., 2013), we suspected that rapid vacuolar volume change might contribute to the ABA hypersensitive stomatal closure in *pat10-1* and *cbl2;cbl3*. To test this hypothesis, we introduced a GFP-translational fusion of the inositol transporter INT1, a tonoplast associated protein (Wolfenstetter et al., 2012), into *pat10-1* and *cbl2;cbl3*. In fully opened guard cells, *pat10-1* and *cbl2;cbl3* contained a mature vacuole that mostly filled the cell (Fig. 4, D, G, and J), comparable to that in the wild type (Fig. 4A). ABA treatment induced a rapid vacuolar convolution in wild type (Fig. 4B), as reported (Gao et al., 2005; Tanaka et al., 2007; Andrés et al., 2014). In comparison, vacuolar convolution upon ABA treatment was more thorough in *pat10-1* (Fig. 4E) and *cbl2;cbl3* (Fig. 4H), resulting in a significantly more convoluted vacuolar structure (Fig. 4, B and J). Washout of ABA recovered vacuolar turgor in all three genetic backgrounds (Fig. 4, C, F, and I), indicating that functional loss of *PAT10* or *CBL2/CBL3* affected only the dynamic remodeling of vacuolar structures but did not cause damage to vacuolar integrity.

To provide further evidence that *pat10-1* and *cbl2;cbl3* are hypersensitive to ABA-induced vacuolar convolution, we stained guard cells with OR Green (OG). OG labeled the vacuolar structures (Supplemental Fig. S5), as reported (Andrés et al., 2014). Indeed, ABA induces a significantly enhanced vacuolar convolution/fragmentation in *pat10-1* and *cbl2;cbl3* compared to that in the wild type (Fig. 4J; Supplemental Fig. S5). These results demonstrate that mutations in *PAT10* or *CBL2/CBL3* result in hypersensitivity to ABA-induced vacuolar convolution and turgor reduction.

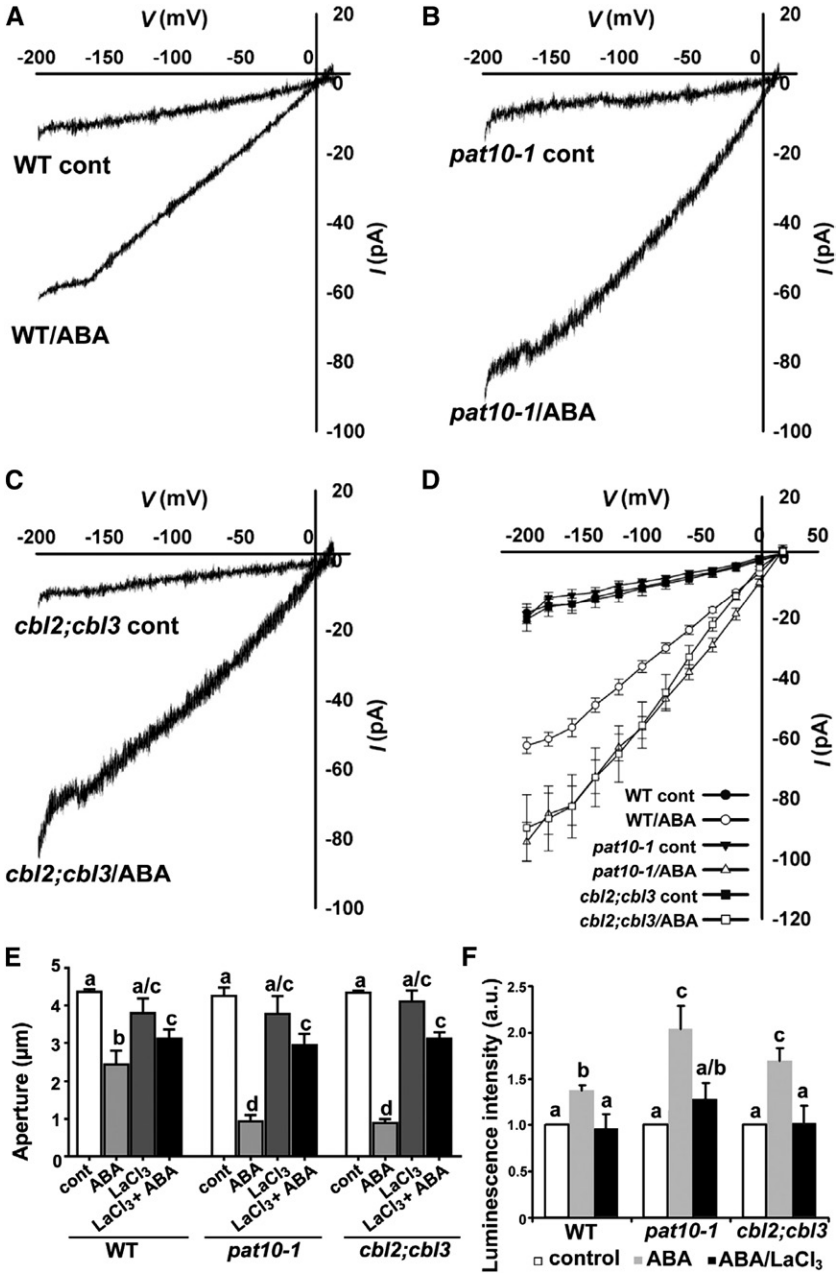

Figure 3. Functional loss of *PAT10* or *CBL2* and *CBL3* resulted in hypersensitivity to ABA-induced Ca^{2+} influx during stomatal movement. A to C, Representative whole-cell Ca^{2+} current recordings from the plasma membrane Ca^{2+}-permeable channels with or without 50 μM ABA treatment in wild-type (A), *pat10-1* (B), or *cbl2;cbl3* (C) guard cell protoplasts. D, Current-voltage relationship (mean ± SD) of whole-cell Ca^{2+} currents recorded in A to C. In total, 9 to 15 guard cells were measured for these genotypes. Means are significantly different between the mutants (*pat10-1* and *cbl2;cbl3*) and the wild type upon ABA treatment (one-way ANOVA, Tukey-Kramer test, $P < 0.05$). E, Stomatal aperture upon control treatment (control), ABA treatment (10 μM ABA), $LaCl_3$ treatment (0.5 mM $LaCl_3$), or ABA plus $LaCl_3$ (10 μM ABA/0.5 mM $LaCl_3$). F, Luminescence intensity of aequorin upon control treatment (control), ABA treatment (ABA), or ABA plus $LaCl_3$ (10 μM ABA/0.5 mM $LaCl_3$). a.u., Arbitrary fluorescent units. In E and F, results are means ± SE of four replicates (20 stomata from two epidermal peels per replicate). Different letters indicate significant difference (one-way ANOVA, Tukey's multiple comparison test, $P < 0.05$).

PAT10 and CBL2/CBL3 Regulate K^+ Homeostasis at the Tonoplast through NHX

Because vacuolar K^+ fluxes are of fundamental importance in the regulation of dynamic vacuolar remodeling during stomatal movement (Gobert et al., 2007; Bassil et al., 2011; Andrés et al., 2014), we suspected that the hypersensitive reduction in the vacuolar volume of *pat10-1* and *cbl2;cbl3* upon ABA

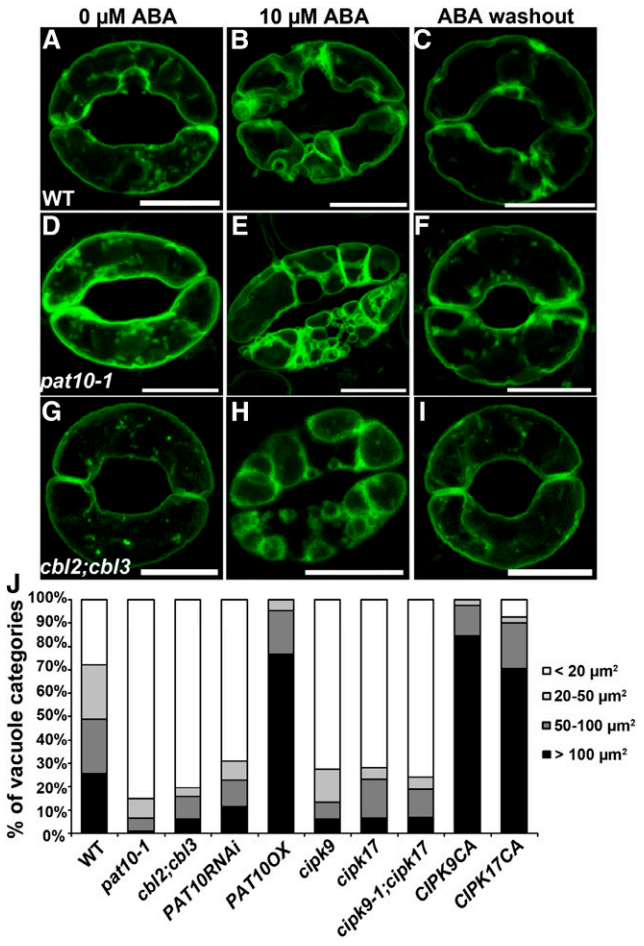

Figure 4. Mutations at *PAT10* and *CBL2/CBL3* resulted in hypersensitivity to ABA-induced vacuolar convolution. A to I, Representative confocal laser scanning microscopy of Pro_{UBQ10}: GFP-INT1 in the wild type (A–C), *pat10-1* (D–F), or *cbl2;cbl3* (G–I) either without ABA (A, D, and G), treated with 10 μM ABA for 2 h (B, E, and H), or treated with 10 μM ABA for 2 h followed by 3 h washout in stomatal opening medium (C, F, and I). J, Vacuolar convolution as indicated by the percentage of visually separate vacuoles at different size range in 12 guard cells. Guard cells were treated with 10 μM ABA for 2 h Bars = 10 μm.

treatment was due to enhanced K^+ efflux or reduced K^+ influx.

To test this hypothesis, we first applied the fungal toxin fusicoccin (FC) during ABA-induced stomatal closure. FC activates H^+-ATPases, causes hyperpolarization of the PM, and thus induces K^+ influx from the PM (Merlot et al., 2007). FC also inhibits K^+ release from the vacuoles of guard cells (MacRobbie and Smyth, 2010; Andrés et al., 2014). FC reversed the effect of ABA in a dosage-dependent manner, i.e. simultaneous application of FC with ABA kept guard cells in an open status both in the wild type and in the mutants (Fig. 5A). However, ABA-induced stomatal closure was completely suppressed by 0.75 μM FC in the wild type, whereas more than 1.25 μM FC was required in *pat10-1* and *cbl2;cbl3* (Fig. 5A), suggesting that the mutants were less sensitive to FC. Similar to the hyposensitivity of *pat10-1* and *cbl2;cbl3* to FC-induced stomatal opening, dynamic vacuolar remodeling also showed the same results (Fig. 5B). Treatment with 0.75 μM FC reversed the effect of ABA on vacuolar fragmentation/convolution in wild-type guard cells, whereas it had little effect on that in *pat10-1* and *cbl2;cbl3* (Fig. 5B). Because enhanced H^+-ATPase activity promotes light-induced stomatal opening (Wang et al., 2013; Kollist et al., 2014) and both *pat10-1* and *cbl2;cbl3* were comparable to the wild type in this process (Fig. 1), the hyposensitive response of the mutants to FC most likely resulted from reduced accumulation of K^+ in their vacuoles. In other words, PAT10 and CBL2/CBL3 might negatively regulate K^+ efflux or positively regulate K^+ influx at the tonoplast upon ABA induction.

To distinguish whether PAT10 and CBL2/CBL3 negatively regulate K^+ efflux or positively regulate K^+ influx at the tonoplast, we took a genetic approach. Arabidopsis TWO PORE K^+ CHANNEL1 (TPK1) mediates vacuolar K^+ release and mutants of TPK1 show

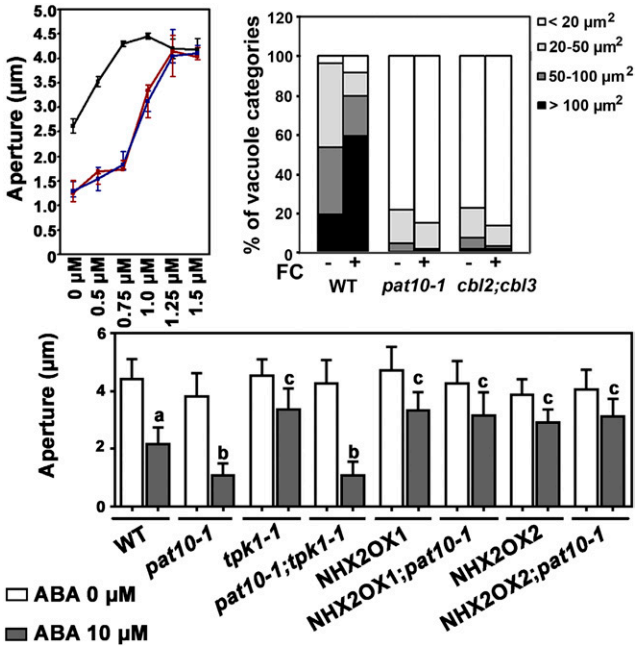

Figure 5. PAT10 and CBL2/CBL3 positively regulate K^+ influx at the tonoplast through NHX. A, Stomatal aperture upon treatment of FC at different concentrations (0–1.5 μM). Black line, wild type; red line, *pat10-1*; blue line, *cbl2;cbl3*. FC was added together with 10 μM ABA to fully opened stomata. Aperture was measured after 2 h treatment. B, Vacuolar convolution as indicated by the percentage of visually separate vacuoles at different size range in 30 guard cells. FC at 0.75 μM was applied together with 10 μM ABA. C, ABA-induced stomatal closure in the wild type, *pat10-1*, *tpk1-1*, *pat10-1;tpk1-1*, NHX2OX1, NHX2OX1;*pat10-1*, NHX2OX2, and NHX2OX2;*pat10-1*. Rosette leaves with preopened stomata were treated with 0 and 10 μM ABA for 2 h before the apertures were measured. Results are means ± SE of four replicates (20 stomata from two epidermal peels per replicate). Different letters indicate significantly different response to ABA-induced stomatal closure (one-way ANOVA, Tukey-Kramer test, $P < 0.05$).

slower stomatal closure upon ABA treatment (Gobert et al., 2007), whereas NHX1 and NHX2 are tonoplast-localized K^+/H^+ exchangers critical for vacuolar accumulation of K^+, whose functional loss results in defective stomatal movement (Bassil et al., 2011; Barragán et al., 2012; Andrés et al., 2014). We introduced *tpk1-1*, a *TPK1* loss-of-function mutant (Gobert et al., 2007), into *pat10-1* to determine their genetic interaction. As reported (Gobert et al., 2007), *tpk1-1* was less sensitive to ABA-induced stomatal closure (Fig. 5C). The *pat10-1;tpk1-1* double mutant showed the same ABA hypersensitivity as *pat10-1* alone (Fig. 5C), suggesting that hypersensitivity of *pat10-1* was not due to defective vacuolar K^+ release. Finally, we generated transgenic lines overexpressing *NHX2*, one of the two functionally interchangeable tonoplast NHXs (Bassil et al., 2011; Barragán et al., 2012). Overexpressing *NHX2* (*NHX2OX*) not only caused slower stomatal closure in the wild type but also in *pat10-1* upon ABA treatment (Fig. 5C). Indeed, both *NHX1* and *NHX2* were transcriptionally downregulated in *pat10-1* and *cbl2;cbl3* with or without ABA treatment, compared to wild type (Supplemental Fig. S6). These results suggest that the hypersensitivity of *pat10-1* to ABA-induced stomatal closure is due to reduced vacuolar K^+ influx, i.e. the PAT10-CBL2/3 system positively regulates K^+ influx at the tonoplast through NHXs.

Tonoplast CIPKs Are Part of the PAT10-CBL Module during ABA-Induced Stomatal Closure

Because CBLs initiate Ca^{2+} signaling by interacting with and activating CIPKs (Gong et al., 2004; Luan, 2009; Batistic et al., 2010), we were interested in determining which CIPKs among the 26 Arabidopsis CIPKs are involved in CBL2/CBL3-mediated ABA signaling during stomatal movement. A guard cell-specific transcriptomic experiment suggested that several CIPKs are highly expressed in guard cells (Bak et al., 2013). One of the guard cell-expressed CIPKs, CIPK9, interacts with CBL2 or CBL3 by yeast two-hybrid analysis and bimolecular fluorescence complementation (BiFC) (Liu et al., 2013; Tang et al., 2015). The expression of *CIPK9* in guard cells was proven earlier by a promoter:reporter analysis (Liu et al., 2013). In addition, *cipk9-1*, a null mutant of *CIPK9* (Pandey et al., 2007), is hypersensitive to ABA during seed germination (Pandey et al., 2004, 2008). *CIPK17* is not only expressed in guard cells, but also responds transcriptionally to osmotic stresses (Zimmermann et al., 2004). We first confirmed the guard cell-enriched expression of *CIPK17* by analyzing histochemical GUS staining of Pro_{CIPK17}:GUS transgenic lines (Supplemental Fig. S7). Interaction between CIPK17 and CBL2 was previously demonstrated by yeast two-hybrid analysis (Tang et al., 2012). We further showed that CIPK17 interacts with both CBL2 and CBL3 at the tonoplast by BiFC and in vitro pull-down assays (Supplemental Fig. S8).

To test whether CIPK9 and CIPK17 were genetic partners of CBL2 and CBL3 in guard cells during ABA responses, we took a reverse genetic approach. We isolated and characterized a T-DNA insertion mutant for *CIPK17* (Fig. 6A), transcript analysis of which identified the mutant allele as a null mutant (Fig. 6B). Both *cipk9-1* and *cipk17* single mutants were hypersensitive to ABA during stomatal closure (Fig. 6C), similar to, but to a lesser extent than, *pat10-1* or *cbl2;cbl3* (Fig. 6C). By crossing, we generated the double mutant of *CIPK9* and *CIPK17* (*cipk9-1;cipk17*) (Fig. 6B), whose ABA sensitivity was comparable to that of *pat10-1* (Fig. 6C). Functional loss of *CIPK9* and *CIPK17* also resulted in a substantial increase in vacuolar fragmentation/convolution upon ABA treatment, similar to that in *pat10-1* or *cbl2;cbl3* (Fig. 4J; Supplemental Fig. S5).

To further verify that CIPK9 and CIPK17 function together with CBL2 and CBL3 in ABA-responsive stomatal movement, we expressed constitutively active (CA) versions of *CIPK9* and *CIPK17*, under Pro_{GC1}, in which the key Thr phosphorylation site within the activation loop was mutated to Asp (Gong et al., 2004). We refer to $CIPK9^{T178D}$ as CIPK9CA and $CIPK17^{T170D}$ as CIPK17CA. The expression of *CIPK9CA* and *CIPK17CA* caused hyposensitivity to ABA-induced stomatal closure in the wild type, in contrast to their loss-of-function mutants (Fig. 6C). Introducing *pat10-1* into either CIPK9CA or CIPK17CA abolished the ABA hyposensitivity

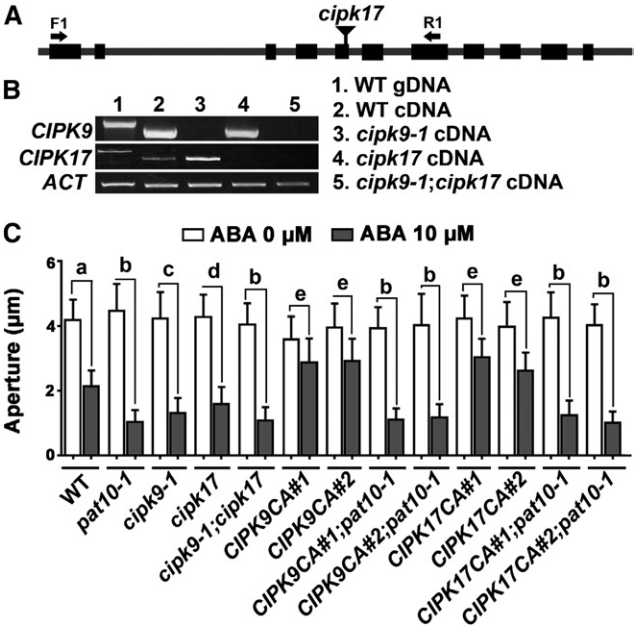

Figure 6. Tonoplast CIPKs are part of the CBL-CIPK module in ABA signaling during stomatal movement. A, Schematic illustration of the *CIPK17* genomic locus with the T-DNA insertion site labeled. B, Transcript analysis verifying the mutant identity of *cipk9-1*, *cipk17*, and the *cipk9-1;cipk17* double mutant. C, Stomatal aperture with or without 2 h 10 μM ABA treatment (ABA or Control). Results are means ± SE (n = 3). For Pro_{GC1}:CIPK9CA and Pro_{GC1}:CIPK17CA, two independent lines were analyzed in either wild-type or *pat10-1* background. Different letters indicate significantly different response to ABA-induced stomatal closure (one-way ANOVA, Tukey-Kramer test, $P < 0.05$).

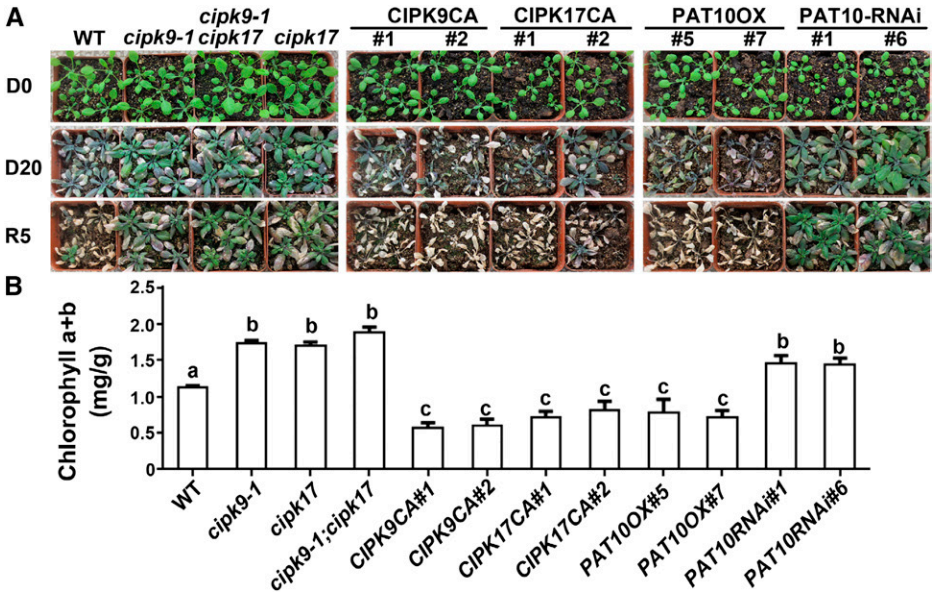

Figure 7. Functional loss of the tonoplast PAT10-CBL-CIPK system in guard cells enhanced drought tolerance. A, A representative drought experiment with the following plants: wild type (WT), *cipk9-1*, *cpik17*, *cipk9-1;cipk17*, CPIK9-CA, CIPK17-CA Pro_{GC1}:PAT10-mRFP, and Pro_{GC1}:PAT10-RNAi. Plants at 20 DAG were stopped watering for 20 d. Images were captured immediately at 20 DAG (D0), after 20 d without watering (D20), or after 5 d rewatering (R5). B, Content of chlorophyll (a + b) in plants at D15. Results shown are means ± SE of three replicates. Different letters indicate significant difference (one-way ANOVA, Tukey-Kramer test, $P < 0.05$).

(Fig. 6C). Instead, CIPK9CA;*pat10-1* and CIPK17CA;*pat10-1* resembled *pat10-1* in their ABA-induced stomatal closure (Fig. 6C). These results demonstrate that CIPK9 and CIPK17 negatively regulate ABA responses during stomatal closure and that they rely on a functional PAT10 to mediate this process.

A given CBL usually interacts with multiple CIPKs to relay Ca^{2+} signaling (D'Angelo et al., 2006; Xu et al., 2006). More CIPKs are expressed in guard cells (Bates et al., 2012), some of which showed an interaction with CBL2 and CBL3, such as CIPK23 (Tang et al., 2015) and CIPK12 (Steinhorst et al., 2015). Therefore, we cannot exclude the possibility that there are more CIPKs interacting with CBL2 and CBL3 at the tonoplast to mediate ABA responses in guard cells. However, because the *cipk9-1;cipk17* double mutant exhibited the same ABA hypersensitivity as *pat10-1* and *cbl2;cbl3* (Fig. 6C), it is highly likely that CIPK9 and CIPK17 are the main CIPKs in this process.

Functional Loss of the Tonoplast PAT10-CBL-CIPK System in Guard Cells Enhances Drought Tolerance

Although functional loss of *CIPK9* and *CIPK17* resulted in ABA hypersensitive stomatal closure, the mutants, either the *cipk9-1* and *cipk17* single mutants or the *cipk9-1;cipk17* double mutant, were developmentally comparable to the wild type (Fig. 7A). To determine whether the ABA hypersensitive stomatal closure was biologically relevant, we tested the behavior of *CIPK* loss- or gain-of-function plants in response to drought because ABA-induced stomatal closure plays a key role in preventing water loss upon drought conditions. We reasoned that faster induction of stomatal closure upon ABA treatment, due to functional loss of the tonoplast PAT10-CBL-CIPK system, would allow plants to better cope with drought. Because *pat10-1* and *cbl2;cbl3* showed developmental defects such as leaf necrosis (Tang et al., 2012; Zhou et al., 2013), we excluded them from the experiments. Instead, we included Pro_{GC1}:PAT10-RNAi and Pro_{GC1}:PAT10-mRFP transgenic lines since the effects would only be due to *PAT10* loss- or gain-of-function in guard cells.

In the drought tolerance experiment, we grew plants under long day condition for 20 d after germination (DAG) with regular watering. Starting from 20 DAG (day 0), watering was stopped for 20 d, during which plants were examined at day 0 and at day 20. After 20 d of drought, plants were watered in equal quantities for 5 d, as described (Nelson et al., 2007). As a consequence of drought, plants of the wild-type, Pro_{GC1}:CIPK9CA, Pro_{GC1}:CIPK17CA, and Pro_{GC1}:PAT10OX genotypes showed extensive leaf necrosis and withering (Fig. 7A). In comparison, rosette leaves of *cipk9-1*, *cipk17*, *cipk9-1;cipk17*, and Pro_{GC1}:PAT10-RNAi showed substantially smaller areas of necrosis and better growth (Fig. 7A). Because chlorophyll content is a good physiological indicator for drought tolerance (Zhao et al., 2016), we analyzed chlorophyll content at 15 d after drought treatment. Consistently, the *cipk9-1*, *cipk17*, and *cipk9-1;cipk17* mutants, as well as Pro_{GC1}:PAT10-RNAi transgenic lines, had a much higher chlorophyll content

than those of the wild type, whereas the Pro_{GC1}:CIPK-9CA, Pro_{GC1}:CIPK17CA, and Pro_{GC1}:PAT10OX transgenic plants had much a lower chlorophyll content (Fig. 7B). Different genotypes were grown in the same tray, so drought tolerance of the *cipk9-1*, *cipk17*, and *cipk9-1; cipk17* mutants, as well as the Pro_{GC1}:PAT10-RNAi transgenic lines, did not result from slower water transpiration. These results demonstrate that functional loss of the PAT10-CBL2/3-CIPK9/17 system in guard cells enhances drought tolerance.

DISCUSSION

We demonstrated here that PAT10 negatively regulates ABA responses during stomatal movement (Fig. 8). Although direct biochemical evidence that PAT10 mediates the *S*-acylation of CBL2 and CBL3 is still lacking, it is highly likely that the role of PAT10 in stomatal movement is mediated through the two CBLs based on the following data: (1) tonoplast association of CBL2 and CBL3 is critical for their functionality (Batistič et al., 2012; Tang et al., 2012) and is dependent on PAT10 (Supplemental Fig. S3); (2) *pat10-1* and *cbl2;cbl3* exhibit the same ABA hypersensitivity during stomatal closure (Figs. 1 and 2); (3) the ABA hyposensitivity of CIPK9CA and CIPK17CA was lost in *pat10-1* (Fig. 6), indicating their genetic epistasis.

Although the PAT10-CBL2/3 system is localized at the tonoplast, we showed that Ca^{2+} influx at the PM and $[Ca^{2+}]_{cyt}$, two early events of ABA signaling in guard cells, were enhanced by their functional loss (Fig. 3; Supplemental Fig. S4). In fact, the PM and the tonoplast are two critical Ca^{2+} signaling platforms connected by the cytoplasm. It was proposed that CIPKs may be shared by PM-associated and tonoplast-associated CBLs, leading to simultaneous formation of CBL-CIPK complexes at different endomembrane compartments within one cell, enabling relay of the Ca^{2+} signal (Batistic et al., 2010; Pittman, 2012). Indeed, in addition to its interaction with the tonoplast-associated CBL2 and CBL3, CIPK9 interacts with two PM-associated CBLs, CBL1 and CBL9 (Kolukisaoglu et al., 2004; Pandey et al., 2007; Batistic et al., 2010), which negatively regulate other ABA-mediated processes (Guo et al., 2002; Pandey et al., 2004, 2008). Two negative regulatory systems mediated by the CBL-CIPK signaling modules at the PM and at the tonoplast may coexist to coordinate the termination of ABA signaling during stomatal movement (Fig. 8).

Previous studies indicated that proton pumps and potassium transporters are likely candidates for the stomatal CBL-CIPK system (Gong et al., 2004; Batistic et al., 2010; Pittman, 2012). Both the PM-associated H-ATPases and the tonoplast-associated V-ATPases have been demonstrated as substrates for the CBL-CIPK modules (Gong et al., 2004; Batelli et al., 2007; Fuglsang et al., 2007). Specifically, *cbl2;cbl3* showed similar developmental defects (Tang et al., 2012) to *vha-a2;vha-3* (Krebs et al., 2010). In addition, vacuolar

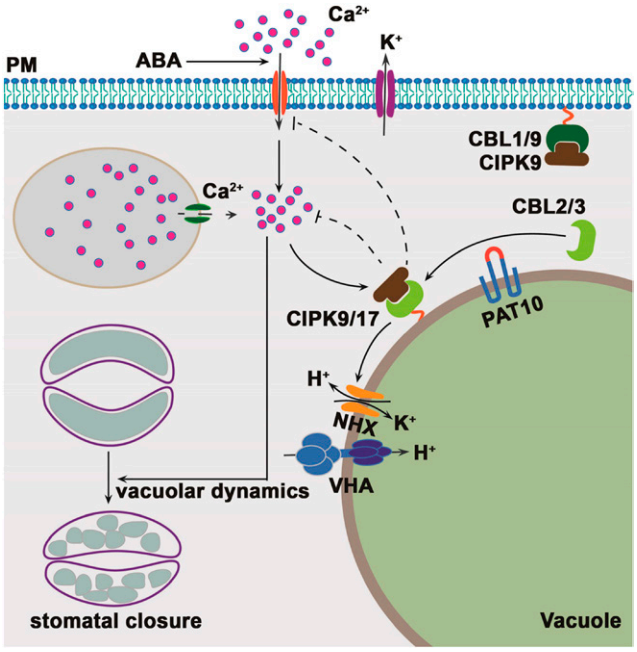

Figure 8. PAT10-mediated tonoplast CBL-CIPK module negatively mediated ABA responses during stomatal movement. During stomatal movement, ABA induces $[Ca^{2+}]_{cyt}$ increase through the PM and possibly also internal Ca^{2+} store. Elevated $[Ca^{2+}]_{cyt}$ initiates ABA-induced stomatal closure, including potassium efflux and vacuolar convolution/fragmentation. Elevated $[Ca^{2+}]_{cyt}$ also promotes the activity of CBL2/3-CIPK9/17, whose association at the tonoplast depends on PAT10. The CBL-CIPK module mediates potassium homeostasis at the tonoplast possibly through NHXs, and by doing so prevents further elevation of $[Ca^{2+}]_{cyt}$.

pH of the *cbl2;cbl3* leaf mesophyll protoplasts was increased, correlating with a reduced V-ATPase activity at the tonoplast (Tang et al., 2012). However, the *vha-a2; vha-a3* double mutant was less sensitive to ABA-induced stomatal closure (Bak et al., 2013), in contrast to *cbl2;cbl3* (Fig. 2). Thus, the ABA hypersensitivity of *cbl2;cbl3* in stomatal movement is unlikely caused by altered V-ATPase activity, as reported recently for their control over Mg^{2+} transport (Tang et al., 2015).

More likely candidates for the tonoplast CBL-CIPK module are the NHX-type K^+/H^+ exchangers. It was shown previously that CIPK24/SOS2-SOS3/CBL4 targets the PM Na^+/H^+ exchanger SOS1/NHX7 (Gong et al., 2004). CBL2 and CBL3 are also implicated in potassium homeostasis (Liu et al., 2013). ABA-hypersensitive stomatal closure and vacuolar convolution of *pat10-1* and *cbl2;cbl3* could result from either enhanced K^+ efflux or reduced K^+ influx at the tonoplast (Figs. 4 and 5). However, *tpk1-1* did not suppress the ABA hypersensitivity of *pat10-1* (Fig. 5), excluding the involvement of enhanced K^+ efflux. By contrast, the PAT10-CBL2/3 system may function by promoting vacuolar accumulation of K^+ through NHXs because overexpressing *NHX2* suppressed the ABA hypersensitivity of *pat10-1* (Fig. 5). Whether the regulation is mediated at the

transcriptional level (Supplemental Fig. S6) or at the posttranslational level will need further investigation.

MATERIALS AND METHODS

Plant Materials and Growth Conditions

The Arabidopsis (*Arabidopsis thaliana*) Columbia-0 ecotype was used as the wild type. The following T-DNA insertion lines were described previously: *pat10-1* (Zhou et al., 2013), *cbl2* (Tang et al., 2012), *cbl3* (Tang et al., 2012), *cipk9-1* (Pandey et al., 2007), and *tpk1-1* (Gobert et al., 2007). The mutant for *CIPK17*, *cipk17* (SALK_062790), was obtained from the ABRC (http://abrc.osu.edu). Arabidopsis plant growth and transformation were as described (Zhou et al., 2013). For drought treatment, plants at 20 DAG were withheld water for 20 d. Chlorophyll (a + b) were extracted from the fourth pair of rosette leaves from plants that were not watered for 15 d. Rewatering was performed as described (Nelson et al., 2007). Measurement was performed as described (Zhao et al., 2016). Histochemical GUS staining was performed as described (Zhou et al., 2013).

Genotyping PCR, RNA Extraction, RT-PCR, and Quantitative Real-Time PCR

The primers used for characterizing the mutant genotypes are as follows: ZP32/ZP1892 for the wild-type copy and ZP33/ZP1 for the mutant copy of *PAT10* in *pat10-1*; ZP2270/ZP2271 for the wild-type copy and ZP2271/ZP1 for the mutant copy of *CBL2* in *cbl2*; ZP2542/ZP2273 for the wild-type copy and ZP2542/ZP4 for the mutant copy of *CBL3* in *cbl3*; ZP1897/ZP1898 for the wild-type copy and ZP1897/ZP1 for the mutant copy of *TPK1* in *tpk1-1*; ZP3926/ZP3927 for the wild-type copy and ZP3927/ZP1 for the mutant copy of *CIPK9* in *cipk9-1*; and ZP4332/ZP4333 for the wild-type copy and ZP4332/ZP1 for the mutant copy of *CIPK17* in *cipk17*.

Total RNA extractions were performed with the Ultrapure RNA extraction kit (CWBIO) according to the manufacturer's instructions. Oligo(dT)-primed cDNAs were synthesized using Superscript III reverse transcriptase with on-column DNase digestion (Invitrogen). The gene-specific primers used for RT-PCRs are ZP983/ZP3479 for *CIPK9*, ZP3482/ZP3483 for the endogenous *CIPK17*, and ZP16/ZP17 for *ACT2*. The gene-specific primers used for quantitative real-time PCR (qPCR) are ZP5423/ZP5424 for *NHX1* and ZP5527/ZP5528 for *NHX2*. qPCR was performed and analyzed as described (Zhou et al., 2013). All primers are listed in Supplemental Table S1.

Plasmid Construction

All constructs were generated using Gateway technology (Invitrogen), except where noted. The entry vectors containing the gene-specific sequences were generated in pENTR/SD/D-TOPO (Invitrogen) with the following primer pairs: ZP195/ZP416 for *PAT10*, ZP1845/ZP1846 for *INT1*, ZP983/ZP3479 for *CIPK9*, ZP3482/ZP3483 for *CIPK17*, and ZP628/ZP629 for *NHX2*. The CA mutations of the CIPKs were generated using a Phusion site-directed mutagenesis kit according to the manufacturer's (ThermoFisher) instructions with the following primers: ZP3874/ZP3875 for *CIPK9CA* and ZP3856/ZP3857 for *CIPK17CA*. The entry vectors for *CBL2* and *CBL3* were described previously (Zhou et al., 2013). Pro_{GC1} (Yang et al., 2008) was amplified using the primer pair ZP2808/ZP2205, which contain *Sac*I/*Spe*I sites, respectively. After enzymatic digestion, the Pro_{GC1} fragment replaced Pro_{LAT52} in Pro_{LAT52}:GW-mRFP (Feng et al., 2016) or Pro_{35S} in Pro_{35S}:RNAi to generate Pro_{GC1}:GW-mRFP or Pro_{GC1}:RNAi, respectively. The Pro_{GC1}:PAT10-RNAi construct was generated by amplifying the PAT10-RNAi fragment with the primer pair ZP3107/ZP3108, digesting with *Bam*HI/*Kpn*I, and ligation with *Bam*HI/*Kpn*I-digested Pro_{GC1}:RNAi. A 3-kb fragment upstream of the *CIPK17* start codon (Pro_{CIPK17}) was amplified with the primer pair ZP4237/ZP4238. The entry vector containing Pro_{CIPK17} was used in an LR reaction with the destination vector pMDC163 (Curtis and Grossniklaus, 2003) to generate the reporter construct Pro_{CIPK17}:GUS. The destination vectors for BiFC, pSITE-nEYFP-N1 and pSITE-cEYFP-N1, were obtained from ABRC. Expression vectors were generated by combining entry vectors with relevant destination vectors in LR reactions using LR Clonase II (Invitrogen). Primers used to generate the *Escherichia coli* expression vectors are ZP3510/ZP3511 for CBL2-His and ZP3512/ZP3513 for CBL3-His. Primers used to generate the entry vector for CIPK17-GFP are ZP3498/ZP3499. All primers are listed in Supplemental Table S1.

Measurement of Stomatal Aperture

For ABA-induced stomatal closure, the youngest fully expanded rosette leaves from plants at 4 weeks after germination (WAG) were floated on stomatal opening buffer containing 5 mM MES, 10 mM KCl, and 50 μM $CaCl_2$ (pH 6.15) for 3 h in the light to preopen stomata. The leaves were subsequently transferred to control buffer (0.1% ethanol, v/v) or buffers containing either 0, 10, or 100 μM ABA for 2.5 h. Epidermal strips of the abaxial side were taken for the measurement of stomatal apertures.

For light-induced stomatal opening, leaves were excised from 4-DAG, 12-h dark-adapted plants and incubated in the opening buffer (30 mM KCl and 10 mM MES-KOH, pH 6.5) for 0.5 h in the dark, 0.5 h before the beginning of the light cycle. Leaves were illuminated for 0, 1, or 2 h before stomatal aperture measurement.

For ABA inhibition of light-induced stomatal opening, leaves were excised from 4-DAG, 12 h-dark-adapted plants and incubated in the opening buffer (30 mM KCl and 10 mM MES-KOH, pH 6.5) for 0.5 h in the dark, 0.5 h before the beginning of the light cycle. The stomatal apertures were measured after the light cycle in the presence of 10 μM ABA buffer or the solvent control buffer (0.1% ethanol, v/v) for 2.5 h

Measurement of Ca^{2+} Influx by Whole-Cell Patch Clamping

Arabidopsis guard cell protoplasts were isolated as described previously (Zhang et al., 2008). Briefly, epidermis was collected from young leaves of 4-WAG plants. Samples were blended in 700 mL of distilled water for 30 s. The peels were filtered through a 100-μm nylon mesh and digested by 5 mL enzyme solution I in a shaking water bath at 120 rpm for 30 min at 28°C. Enzyme solution I contains 0.7% (w/v) cellulysin cellulase, 0.1% (w/v) PVP 40, and 0.25% (w/v) BSA in 55% (v/v) basic solution (5 mM MES, 0.5 mM $CaCl_2$, 0.5 mM $MgCl_2$, 0.5 mM VC, 10 μM KH_2PO_4, and 0.5 mM sorbitol, pH 5.5). Then, 5 mL of basic solution was added and samples were shaken for another 8 min. The partially digested peels were collected through a 100-μm nylon mesh and put into 5 mL of enzyme solution II (1.5% Onuzuka cellulase RS, 0.02% [w/v] cellulase Y-23, and 0.25% [w/v] BSA in 100% [v/v] basic solution) for digestion at 60 rpm for 20 to 30 min at 25°C. Then, the peels were mixed by pipetting up and down with a 1-mL pipette and filtered through 30-μm nylon mesh. The protoplasts were centrifuged at 800 rpm for 5 min and washed twice with basic solution (Zhang et al., 2008).

Patch clamp electrophysiology was performed using previously established techniques (Mori et al., 2006). For Ca^{2+} current recording, the bath solution contained 50 mM $BaCl_2$, 0.1 mM DTT, and 10 mM MES-Tris (pH 5.6), with osmolality of 540 mOSM, and the pipette solutions contained 10 mM $BaCl_2$, 2 mM EGTA, 0.1 mM DTT, and 10 mM HEPES (pH 7.5), with osmolality of 560 mOSM. The whole-cell currents were recorded using an Axopatch-200B amplifier (Axon Instruments) after the whole-cell configuration was achieved. The holding potential was −13 mV and voltage ramps were from −200 to +20 mV. For ABA treatment, 50 μM ABA was added to the bath solution after achieving the whole-cell configuration and currents were collected 10 min after ABA application. pCLAMP software (version 10.2; Axon Instruments) was used to acquire and analyze the whole-cell currents. SigmaPlot 11.0 software was used to draw current-voltage plots and for data analysis.

Pharmacological Treatment

To test the effect of $LaCl_3$, the youngest fully expanded rosette leaves from plants at 4 WAG were floated on the opening buffer containing 5 mM MES, 10 mM KCl, and 50 μM $CaCl_2$ (pH 6.15) for 3 h in the light to preopen stomata. Samples were subsequently transferred to a buffer containing 0, 10, or 10 μM ABA with 0.5 mM $LaCl_3$ for 2.5 h before the measurement of stomatal aperture.

To test the effect of EGTA, label vacuoles with OG, or test the effect of FC, the youngest fully expanded rosette leaves from 4-WAG plants were first floated on opening buffer containing 5 mM MES, 10 mM KCl, and 50 μM $CaCl_2$ (pH 6.15) for 3 h in the light to preopen stomata. To test the effect of EGTA, samples were subsequently transferred to a buffer containing 0, 10, or 10 μM ABA with 0.1 mM EGTA for 2.5 h before measurement of the stomatal aperture.

For labeling vacuoles with OG, the lower epidermis of the samples was torn and dipped in opening buffer with 10 μM OG for 30 min and then subsequently transferred to a buffer containing 0 μM ABA or 10 μM ABA for 2.5 h To test the effect of FC, samples were subsequently transferred to a buffer containing 0, 10, or 10 μM ABA with different FC concentrations (0.5, 0.75, 1, 1.25, and 1.5 μM) for 2.5 h before measurement of the stomatal aperture.

Biochemical Assays

Cell fractionation and western blot analysis as shown in Supplemental Figure S3 were performed as described (Chai et al., 2016; Wan et al., 2017). For the in vitro pull-down assay shown in Supplemental Figure S8, the plasmids expressing CBL2-His, CBL3-His, or His were transformed into BL21 (Rosetta). Target proteins were induced by 0.8 mM IPTG for 12 to 18 h at 16°C. The recombinant proteins were affinity-purified according to the manufacturer's protocol (GE Healthcare Life Science) and analyzed by SDS-PAGE. For CIPK17-GFP, leaves of the Pro_{35S}:CIPK17-GFP transgenic plants were homogenized in liquid nitrogen and extracted in 1 mL of pull-down buffer (40 mM Tris-HCl, pH 7.5, 100 mM NaCl, 1 mM Na_2-EDTA, 5% glycerol, 1 mM PMSF, and protease inhibitor mixture [Roche]) supplemented with 0.75% Triton X-100. Proteins were extracted at 4°C with mixing for 15 min. The debris was removed by centrifugation at top speed in a microcentrifuge tube for 10 min at 4°C. The supernatant was applied to anti-GFP mAb-magnetic agarose (MBL) for 2 h at 4°C and then washed thoroughly four to five times with 1 mL of pull-down buffer per wash. The anti-GFP mAb-magnetic agarose containing CIPK17-GFP was used as bait in the pull-down assays. Pull-down assays were carried out by incubating CBL2-His, CBL3-His, or His with the anti-GFP mAb-magnetic agarose containing CIPK17-GFP at 4°C for 2 h. The agarose was then washed five times with pull-down buffer. Proteins bound to the agarose were eluted in SDS-PAGE loading buffer, boiled for 10 min, and applied to 12% SDS-PAGE for western-blot analysis. Anti-actin (#HC201), anti-His (#501), and anti-GFP (#HT801) antibodies were purchased from Transgen.

Quantification of Vacuoles

The areas of visibly individual vacuoles, imaged by INT1-GFP labeling or OG staining, were measured by Image J. Vacuoles were classified into four categories based on their area, i.e. below 20 μm^2, 20 to 50 μm^2, 50 to 100 μm^2, and over 100 μm^2. In total, 30 pairs of guard cells were measured for each genotype or treatment.

BiFC and Fluorescent Microscopy

BiFC was performed as described (Zhou et al., 2013; Feng et al., 2016). Luminescence intensity of aequorin, indicating the Ca^{2+} concentration in the cytoplasm as described (Mehlmer et al., 2012), upon control treatment, ABA treatment (10 μM ABA), or ABA plus $LaCl_3$ (10 μM ABA/0.5 mM $LaCl_3$) was measured by Image J. In total, luminescence signals from 25 pairs of guard cells from five plants were measured for each genotype or treatment. Microscopy imaging was performed either by using a Leica TCS SP5 (Leica) or a Zeiss LSM880 (Zeiss) confocal laser-scanning microscope with a 488-nm argon laser/band-pass 505- to 550-nm filter for GFP and a 561-nm laser/band-pass 600- to 650-nm filter for RFP. Images were processed using Adobe Photoshop CS3 (Adobe).

Accession Numbers

Sequence data from this article can be found in the GenBank databases under the following accession numbers: At3g51390 for *PAT10*; At5g55990 for *CBL2*; At4g26570 for *CBL3*; At4g17615 for *CBL1*; At4g24400 for *CIPK8*; At1g01140 for *CIPK9*; At1g48260 for *CIPK17*; At1g22690 for *GC1*; At2g43330 for *INT1*; At5g27150 for *NHX1*; At3g05030 for *NHX2*; and At5g55630 for *TPK1*.

Supplemental Data

The following supplemental materials are available.

Supplemental Figure S1. Manipulating *PAT10* expression in mature guard cells altered ABA sensitivity during stomatal movement.

Supplemental Figure S2. Loss of function of *CBL2* or *CBL3* alone did not affect ABA-induced stomatal closure.

Supplemental Figure S3. The tonoplast association of CBL2 is abolished in *pat10-1* guard cells.

Supplemental Figure S4. EGTA suppressed the hypersensitivity of *pat10-1* and *cbl2;cbl3* to ABA-induced stomatal closure.

Supplemental Figure S5. Mutations at the PAT10-CBL2/CBL3-CIPK module resulted in hypersensitivity to ABA-induced vacuolar convolution.

Supplemental Figure S6. *NHX1* and *NHX2* were transcriptionally down-regulated in *pat10-1* and *cbl2;cbl3*.

Supplemental Figure S7. *CIPK17* is highly expressed in mature guard cells.

Supplemental Figure S8. CIPK17 interacts with CBL2 and CBL3 but not CBL1.

Supplemental Table S1. Oligos used in the study.

ACKNOWLEDGMENTS

We thank the ABRC for the described T-DNA insertion lines.

Received March 30, 2018; accepted June 5, 2018; published June 13, 2018.

LITERATURE CITED

Andrés Z, Pérez-Hormaeche J, Leidi EO, Schlücking K, Steinhorst L, McLachlan DH, Schumacher K, Hetherington AM, Kudla J, Cubero B, Pardo JM (2014) Control of vacuolar dynamics and regulation of stomatal aperture by tonoplast potassium uptake. Proc Natl Acad Sci USA **111**: E1806–E1814

Bak G, Lee EJ, Lee Y, Kato M, Segami S, Sze H, Maeshima M, Hwang JU, Lee Y (2013) Rapid structural changes and acidification of guard cell vacuoles during stomatal closure require phosphatidylinositol 3,5-bisphosphate. Plant Cell **25**: 2202–2216

Barragán V, Leidi EO, Andrés Z, Rubio L, De Luca A, Fernández JA, Cubero B, Pardo JM (2012) Ion exchangers NHX1 and NHX2 mediate active potassium uptake into vacuoles to regulate cell turgor and stomatal function in *Arabidopsis*. Plant Cell **24**: 1127–1142

Bassil E, Tajima H, Liang YC, Ohto MA, Ushijima K, Nakano R, Esumi T, Coku A, Belmonte M, Blumwald E (2011) The *Arabidopsis* Na+/H+ antiporters NHX1 and NHX2 control vacuolar pH and K+ homeostasis to regulate growth, flower development, and reproduction. Plant Cell **23**: 3482–3497

Batelli G, Verslues PE, Agius F, Qiu Q, Fujii H, Pan S, Schumaker KS, Grillo S, Zhu JK (2007) SOS2 promotes salt tolerance in part by interacting with the vacuolar H+-ATPase and upregulating its transport activity. Mol Cell Biol **27**: 7781–7790

Bates GW, Rosenthal DM, Sun J, Chattopadhyay M, Peffer E, Yang J, Ort DR, Jones AM (2012) A comparative study of the *Arabidopsis thaliana* guard-cell transcriptome and its modulation by sucrose. PLoS One **7**: e49641

Batistic O, Waadt R, Steinhorst L, Held K, Kudla J (2010) CBL-mediated targeting of CIPKs facilitates the decoding of calcium signals emanating from distinct cellular stores. Plant J **61**: 211–222

Batistič O, Rehers M, Akerman A, Schlücking K, Steinhorst L, Yalovsky S, Kudla J (2012) S-acylation-dependent association of the calcium sensor CBL2 with the vacuolar membrane is essential for proper abscisic acid responses. Cell Res **22**: 1155–1168

Blatt MR (2000) Ca(2+) signalling and control of guard-cell volume in stomatal movements. Curr Opin Plant Biol **3**: 196–204

Brandt B, Munemasa S, Wang C, Nguyen D, Yong T, Yang PG, Poretsky E, Belknap TF, Waadt R, Aleman F, Schroeder JI (2015) Calcium specificity signaling mechanisms in abscisic acid signal transduction in *Arabidopsis* guard cells. eLife **4**: 10.7554/eLife.03599

Chai S, Ge FR, Feng QN, Li S, Zhang Y (2016) *PLURIPETALA* mediates ROP2 localization and stability in parallel to *SCN1* but synergistically with *TIP1* in root hairs. Plant J **86**: 413–425

Cheong YH, Pandey GK, Grant JJ, Batistic O, Li L, Kim BG, Lee SC, Kudla J, Luan S (2007) Two calcineurin B-like calcium sensors, interacting with protein kinase CIPK23, regulate leaf transpiration and root potassium uptake in Arabidopsis. Plant J **52**: 223–239

Curtis MD, Grossniklaus U (2003) A gateway cloning vector set for high-throughput functional analysis of genes in planta. Plant Physiol **133**: 462–469

D'Angelo C, Weinl S, Batistic O, Pandey GK, Cheong YH, Schültke S, Albrecht V, Ehlert B, Schulz B, Harter K, (2006) Alternative complex formation of the Ca-regulated protein kinase CIPK1 controls abscisic acid-dependent and independent stress responses in Arabidopsis. Plant J **48**: 857–872

Feng QN, Kang H, Song SJ, Ge FR, Zhang YL, Li E, Li S, Zhang Y (2016) Arabidopsis RhoGDIs are critical for cellular homeostasis of pollen tubes. Plant Physiol **170**: 841–856

Finkelstein R (2013) Abscisic Acid synthesis and response. Arabidopsis Book **11**: e0166

Fuglsang AT, Guo Y, Cuin TA, Qiu Q, Song C, Kristiansen KA, Bych K, Schulz A, Shabala S, Schumaker KS, Palmgren MG, Zhu JK (2007) Arabidopsis protein kinase PKS5 inhibits the plasma membrane H+-ATPase by preventing interaction with 14-3-3 protein. Plant Cell **19**: 1617–1634

Gao XQ, Li CG, Wei PC, Zhang XY, Chen J, Wang XC (2005) The dynamic changes of tonoplasts in guard cells are important for stomatal movement in *Vicia faba*. Plant Physiol **139**: 1207–1216

Gobert A, Isayenkov S, Voelker C, Czempinski K, Maathuis FJ (2007) The two-pore channel *TPK1* gene encodes the vacuolar K+ conductance and plays a role in K+ homeostasis. Proc Natl Acad Sci USA **104**: 10726–10731

Gong D, Guo Y, Schumaker KS, Zhu JK (2004) The SOS3 family of calcium sensors and SOS2 family of protein kinases in Arabidopsis. Plant Physiol **134**: 919–926

Guo Y, Halfter U, Ishitani M, Zhu JK (2001) Molecular characterization of functional domains in the protein kinase SOS2 that is required for plant salt tolerance. Plant Cell **13**: 1383–1400

Guo Y, Xiong L, Song CP, Gong D, Halfter U, Zhu JK (2002) A calcium sensor and its interacting protein kinase are global regulators of abscisic acid signaling in *Arabidopsis*. Dev Cell **3**: 233–244

Hauser F, Waadt R, Schroeder JI (2011) Evolution of abscisic acid synthesis and signaling mechanisms. Curr Biol **21**: R346–R355

Hetherington AM (2001) Guard cell signaling. Cell **107**: 711–714

Himmelbach A, Yang Y, Grill E (2003) Relay and control of abscisic acid signaling. Curr Opin Plant Biol **6**: 470–479

Kim TH, Böhmer M, Hu H, Nishimura N, Schroeder JI (2010) Guard cell signal transduction network: advances in understanding abscisic acid, CO2, and Ca2+ signaling. Annu Rev Plant Biol **61**: 561–591

Kollist H, Nuhkat M, Roelfsema MR (2014) Closing gaps: linking elements that control stomatal movement. New Phytol **203**: 44–62

Kolukisaoglu U, Weinl S, Blazevic D, Batistic O, Kudla J (2004) Calcium sensors and their interacting protein kinases: genomics of the Arabidopsis and rice CBL-CIPK signaling networks. Plant Physiol **134**: 43–58

Krebs M, Beyhl D, Görlich E, Al-Rasheid KA, Marten I, Stierhof YD, Hedrich R, Schumacher K (2010) Arabidopsis V-ATPase activity at the tonoplast is required for efficient nutrient storage but not for sodium accumulation. Proc Natl Acad Sci USA **107**: 3251–3256

Liu LL, Ren HM, Chen LQ, Wang Y, Wu WH (2013) A protein kinase, calcineurin B-like protein-interacting protein Kinase9, interacts with calcium sensor calcineurin B-like Protein3 and regulates potassium homeostasis under low-potassium stress in *Arabidopsis*. Plant Physiol **161**: 266–277

Luan S (2009) The CBL-CIPK network in plant calcium signaling. Trends Plant Sci **14**: 37–42

MacRobbie EA, Smyth WD (2010) Effects of fusicoccin on ion fluxes in guard cells. New Phytol **186**: 636–647

Mehlmer N, Parvin N, Hurst CH, Knight MR, Teige M, Vothknecht UC (2012) A toolset of aequorin expression vectors for *in planta* studies of subcellular calcium concentrations in *Arabidopsis thaliana*. J Exp Bot **63**: 1751–1761

Merlot S, Leonhardt N, Fenzi F, Valon C, Costa M, Piette L, Vavasseur A, Genty B, Boivin K, Müller A, Giraudat J, Leung J (2007) Constitutive activation of a plasma membrane H(+)-ATPase prevents abscisic acid-mediated stomatal closure. EMBO J **26**: 3216–3226

Mori IC, Murata Y, Yang Y, Munemasa S, Wang YF, Andreoli S, Tiriac H, Alonso JM, Harper JF, Ecker JR, Kwak JM, Schroeder JI (2006) CDPKs CPK6 and CPK3 function in ABA regulation of guard cell S-type anion- and Ca(2+)-permeable channels and stomatal closure. PLoS Biol **4**: e327

Nelson DE, Repetti PP, Adams TR, Creelman RA, Wu J, Warner DC, Anstrom DC, Bensen RJ, Castiglioni PP, Donnarummo MG, (2007) Plant nuclear factor Y (NF-Y) B subunits confer drought tolerance and lead to improved corn yields on water-limited acres. Proc Natl Acad Sci USA **104**: 16450–16455

Pandey GK, Cheong YH, Kim KN, Grant JJ, Li L, Hung W, D'Angelo C, Weinl S, Kudla J, Luan S (2004) The calcium sensor calcineurin B-like 9 modulates abscisic acid sensitivity and biosynthesis in Arabidopsis. Plant Cell **16**: 1912–1924

Pandey GK, Cheong YH, Kim BG, Grant JJ, Li L, Luan S (2007) CIPK**9**: a calcium sensor-interacting protein kinase required for low-potassium tolerance in *Arabidopsis*. Cell Res **17**: 411–421

Pandey GK, Grant JJ, Cheong YH, Kim BG, Li G, Luan S (2008) Calcineurin-B-like protein CBL9 interacts with target kinase CIPK3 in the regulation of ABA response in seed germination. Mol Plant **1**: 238–248

Pei ZM, Murata Y, Benning G, Thomine S, Klüsener B, Allen GJ, Grill E, Schroeder JI (2000) Calcium channels activated by hydrogen peroxide mediate abscisic acid signalling in guard cells. Nature **406**: 731–734

Pittman JK (2012) Multiple transport pathways for mediating intracellular pH homeostasis: the contribution of H+/ion exchangers. Front Plant Sci **3**: 11

Steinhorst L, Mähs A, Ischebeck T, Zhang C, Zhang X, Arendt S, Schültke S, Heilmann I, Kudla J (2015) Vacuolar CBL-CIPK12 Ca(2+)-sensor-kinase complexes are required for polarized pollen tube growth. Curr Biol **25**: 1475–1482

Tanaka Y, Kutsuna N, Kanazawa Y, Kondo N, Hasezawa S, Sano T (2007) Intra-vacuolar reserves of membranes during stomatal closure: the possible role of guard cell vacuoles estimated by 3-D reconstruction. Plant Cell Physiol **48**: 1159–1169

Tang R-J, Liu H, Yang Y, Yang L, Gao X-S, Garcia VJ, Luan S, Zhang H-X (2012) Tonoplast calcium sensors CBL2 and CBL3 control plant growth and ion homeostasis through regulating V-ATPase activity in *Arabidopsis*. Cell Res **22**: 1650–1665

Tang RJ, Zhao FG, Garcia VJ, Kleist TJ, Yang L, Zhang HX, Luan S (2015) Tonoplast CBL-CIPK calcium signaling network regulates magnesium homeostasis in Arabidopsis. Proc Natl Acad Sci USA **112**: 3134–3139

Wan ZY, Chai S, Ge FR, Feng QN, Zhang Y, Li S (2017) Arabidopsis PROTEIN S-ACYL TRANSFERASE4 mediates root hair growth. Plant J **90**: 249–260

Wang Y, Chen ZH, Zhang B, Hills A, Blatt MR (2013) PYR/PYL/RCAR abscisic acid receptors regulate K+ and Cl- channels through reactive oxygen species-mediated activation of Ca2+ channels at the plasma membrane of intact Arabidopsis guard cells. Plant Physiol **163**: 566–577

Wolfenstetter S, Wirsching P, Dotzauer D, Schneider S, Sauer N (2012) Routes to the tonoplast: the sorting of tonoplast transporters in *Arabidopsis* mesophyll protoplasts. Plant Cell **24**: 215–232

Xu J, Li HD, Chen LQ, Wang Y, Liu LL, He L, Wu WH (2006) A protein kinase, interacting with two calcineurin B-like proteins, regulates K+ transporter AKT1 in *Arabidopsis*. Cell **125**: 1347–1360

Yang Y, Costa A, Leonhardt N, Siegel RS, Schroeder JI (2008) Isolation of a strong *Arabidopsis* guard cell promoter and its potential as a research tool. Plant Methods **4**: 6

Ye W, Muroyama D, Munemasa S, Nakamura Y, Mori IC, Murata Y (2013) Calcium-dependent protein kinase CPK6 positively functions in induction by yeast elicitor of stomatal closure and inhibition by yeast elicitor of light-induced stomatal opening in Arabidopsis. Plant Physiol **163**: 591–599

Zhang W, Nilson SE, Assmann SM (2008) Isolation and whole-cell patch clamping of Arabidopsis guard cell protoplasts. CSH Protoc **2008**: pdb.prot5014

Zhang W, Jeon BW, Assmann SM (2011) Heterotrimeric G-protein regulation of ROS signalling and calcium currents in *Arabidopsis* guard cells. J Exp Bot **62**: 2371–2379

Zhang YL, Li E, Feng QN, Zhao XY, Ge FR, Zhang Y, Li S (2015) Protein palmitoylation is critical for the polar growth of root hairs in *Arabidopsis*. BMC Plant Biol **15**: 50

Zhao XY, Wang JG, Song SJ, Wang Q, Kang H, Zhang Y, Li S (2016) Precocious leaf senescence by functional loss of PROTEIN S-ACYL TRANSFERASE14 involves the NPR1-dependent salicylic acid signaling. Sci Rep **6**: 20309

Zhou LZ, Li S, Feng QN, Zhang YL, Zhao X, Zeng YL, Wang H, Jiang L, Zhang Y (2013) Protein S-ACYL Transferase10 is critical for development and salt tolerance in *Arabidopsis*. Plant Cell **25**: 1093–1107

Zimmermann P, Hirsch-Hoffmann M, Hennig L, Gruissem W (2004) GENEVESTIGATOR. Arabidopsis microarray database and analysis toolbox. Plant Physiol **136**: 2621–2632

Zou JJ, Li XD, Ratnasekera D, Wang C, Liu WX, Song LF, Zhang WZ, Wu WH (2015) Arabidopsis CALCIUM-DEPENDENT PROTEIN KINASE8 and CATALASE3 function in abscisic acid-mediated signaling and H2O2 homeostasis in stomatal guard cells under drought stress. Plant Cell **27**: 1445–1460